

## RESEARCH ARTICLE

# Lectin-anticancer peptide fusion demonstrates a significant cancer-cell-selective cytotoxic effect and inspires the production of “clickable” anticancer peptide in *Escherichia coli*

Rajeev Pasupuleti<sup>1,2</sup> | Sabrina Riedl<sup>3,4,5</sup> | Laia Saltor Núñez<sup>6</sup> |  
 Marianna Karava<sup>2</sup> | Vajinder Kumar<sup>6</sup>  | Robert Kourist<sup>2</sup> |  
 W. Bruce Turnbull<sup>6</sup> | Dagmar Zweytick<sup>3,4,5</sup> | Birgit Wiltschi<sup>1,2,5,7</sup> 

<sup>1</sup>acib - Austrian Centre of Industrial Biotechnology, Graz, Austria

<sup>2</sup>Institute of Molecular Biotechnology, Graz University of Technology, Graz, Austria

<sup>3</sup>Institute of Molecular Biosciences, Biophysics Division, University of Graz, Graz, Austria

<sup>4</sup>BioHealth, University of Graz, Graz, Austria

<sup>5</sup>BioTechMed-Graz, Graz, Austria

<sup>6</sup>School of Chemistry and Astbury Centre for Structural Molecular Biology, University of Leeds, Leeds, UK

<sup>7</sup>Institute of Bioprocess Science and Engineering, Department of Biotechnology, University of Natural Resources and Life Sciences, Vienna, Austria

## Correspondence

Dagmar Zweytick, Institute of Molecular Biosciences, University of Graz, Humboldtstrasse 50/III, 8010 Graz, Austria.  
 Email: [dagmar.zweytick@uni-graz.at](mailto:dagmar.zweytick@uni-graz.at)

Birgit Wiltschi, acib GmbH & Institute of Bioprocess Science and Engineering, Department of Biotechnology, University of Natural Resources and Life Sciences, Muthgasse, 18, 1190 Vienna, Austria.  
 Email: [birgit.wiltschi@boku.ac.at](mailto:birgit.wiltschi@boku.ac.at)

## Funding information

European Union's Horizon 2020 research and innovation program under the Marie Skłodowska-Curie grants, Grant/Award Numbers: 746421, 814029; BMK, BMDW, SFG, Standortagentur Tirol, Government of Lower Austria und Vienna Business Agency in the framework of COMET—Competence Centers for Excellent Technologies. The COMET-Funding Program is managed by the Austrian Research Promotion Agency FFG, Grant/Award Number: 872161;

## Abstract

Targeted killing of tumor cells while protecting healthy cells is the pressing priority in cancer treatment. Lectins that target a specific glycan marker abundant in cancer cells can be valuable new tools for selective cancer cell killing. The lectin Shiga-like toxin 1 B subunit (Stx1B) is an example that specifically binds globotriaosylceramide (CD77 or Gb3), which is overexpressed in certain cancers. In this study, a human lactoferricin-derived synthetic retro di-peptide R-DIM-P-LF11-215 with antitumor efficacy was fused to the lectin Stx1B to selectively target and kill Gb3+ cancer cells. We produced lectin-peptide fusion proteins in *Escherichia coli*, isolated them by Gb3-affinity chromatography, and assessed their ability to selectively kill Gb3+ cancer cells in a Calcein AM assay. Furthermore, to expand the applications of R-DIM-P-LF11-215 in developing therapeutic bioconjugates, we labeled R-DIM-P-LF11-215 with the unique reactive non-canonical amino acid N<sup>ε</sup>-((2-azidoethoxy)carbonyl)-L-lysine (AzK) at a selected position by amber stop codon suppression. The R-DIM-P-LF11-215 20AzK and the unlabeled R-DIM-P-LF11-215 parent peptide were produced as GST-fusion proteins for soluble expression in *E. coli* for the first time. We purified both variants by size-exclusion chromatography and

**Reviewing Editor:** John Kuriyan

This is an open access article under the terms of the [Creative Commons Attribution-NonCommercial-NoDerivs](https://creativecommons.org/licenses/by-nc-nd/4.0/) License, which permits use and distribution in any medium, provided the original work is properly cited, the use is non-commercial and no modifications or adaptations are made.

© 2023 The Authors. *Protein Science* published by Wiley Periodicals LLC on behalf of The Protein Society.

Austrian Research Promotion Agency,  
Grant/Award Number: 855671; University  
of Natural Resources and Life Sciences  
Vienna (BOKU)

analyzed their peptide masses. Finally, a cyanin 3 fluorophore was covalently conjugated to R-DIM-P-LF11-215 20AzK by strain-promoted alkyne-azide cycloaddition. Our results showed that the recombinant lectin-peptide fusion R-DIM-P-LF11-215-Stx1B killed >99% Gb3+ HeLa cells while Gb3-negative cells were unaffected. The peptides R-DIM-P-LF11-215 and R-DIM-P-LF11-215 20AzK were produced recombinantly in *E. coli* in satisfactory amounts and were tested functional by cytotoxicity and cell-binding assays, respectively.

#### KEYWORDS

anticancer peptide, click chemistry, fusion proteins, human lactoferricin-derived peptide, peptide purification, recombinant peptide production, targeted drug delivery

## 1 | INTRODUCTION

Recent advances in targeted drug delivery with conjugates comprising monoclonal antibodies as carriers and small molecules and peptides as drugs have created a niche for the next generation of cancer therapy research (Baudino, 2015). The advantages of targeted therapy are enhanced efficacy, lower toxicity, and greater specificity for cancer cells without affecting normal cells. Despite remarkable progress in developing novel combinations of multi-component targeted drugs, challenges of drug resistance with antibody-drug conjugates and small-molecule drugs still need to be addressed (Nejadmoghaddam et al., 2019; Zhong et al., 2021). Alternatively, peptides with anticancer potential are less prone to drug resistance and are easy to conjugate to drug carriers (Deslouches & Di, 2017; Ko & Maynard, 2018; Xie et al., 2020). More than 20 anticancer peptides (ACPs) have been approved by the United States Food and Drug Administration (FDA) as of 2019 (Pan et al., 2020) and therefore ACPs continue to be an active area of research in cancer therapy. In this context, peptides derived from the bovine and human glycoprotein lactoferrin with antitumor properties are a special focus of cancer drug development (Barragán-Cárdenas et al., 2022; Guerra et al., 2019).

Anticancer peptides can be classified based on their structure as  $\alpha$ -helical,  $\beta$ -pleated sheets, cyclic, and random coils (Pan et al., 2020; Xie et al., 2020). One of the mixed structured ( $\alpha$ -helical and  $\beta$ -sheet) cationic amphipathic peptides is human lactoferricin (hLFcin), which constitutes amino acids 1–46 from the N-terminal region of human lactoferrin (hLF) (Gifford et al., 2005). Based on the residues 21–31 of hLFcin, LF11 peptide variants were synthesized (Zweytick et al., 2006). The LF11 peptides (patent, Antitumor Peptides: PCT/EP2014/050330; US 14/760,445; EP 14700349.5) exhibited antitumor activity by binding exposed phosphatidylserine (PS) which is a cancer-specific antigen on glioblastoma, melanoma and rhabdomyosarcoma (Grissenberger et al., 2020; Maxian et al., 2021; Riedl

et al., 2011; Riedl et al., 2014; Riedl et al., 2015; Riedl et al., 2017; Wodlej et al., 2019; Wußmann et al., 2022). Recently, Zweytick and co-workers compared seven LF11-derived synthetic peptides for antitumor efficacy (Grissenberger et al., 2020). The authors reported the synthetic peptide R-DIM-P-LF11-215 (hereafter RDP215) to be highly active when tested on glioblastoma and melanoma cell lines in 2D models as well as on melanoma in 3D tumor models (Grissenberger et al., 2020; Maxian et al., 2021). The initial interaction of RDP215 and related peptides with PS specifically exposed by cancer plasma membranes is reported to be based on the electrostatic attraction of the cationic RDP215 peptide with the anionic PS phospholipid (Riedl et al., 2011). Specific entry into cancer cells is enabled by the amphipathic character of the peptides and leads to subsequent interaction with intracellular targets such as negatively charged lipids of the Golgi or mitochondria, that finally leads to induction of cell death by apoptosis (Maxian et al., 2021; Riedl et al., 2015; Wodlej et al., 2019).

The peptide RDP215 is interesting because it performs the dual function of binding to cancer cells and killing them. However, the exposure levels of PS differ in the tumor microenvironment of a variety of cancer types (Desai et al., 2016; Ran et al., 2002; Stafford & Thorpe, 2011). This poses a challenge when treating multiple tumors with differential PS exposure in an individual or in metastasis where the bioavailability or payloads of the peptide become low at some tumor sites. Peptide RDP215 has been used as a single-agent drug until now. A study by Law and colleagues observed that kla peptide linked to a cell-penetrating peptide r7 showed better cytotoxicity on human fibrosarcoma cell line HT1080 than kla peptide alone (Law et al., 2006). Hence, to improve the RDP215 bioavailability in the tumor site, we intended to produce a bispecific fusion of RDP215. We decided to genetically fuse RDP215 to the lectin Stx1B that selectively binds overexpressed globotriaosylceramide (Gb3) on cancer cells. Stx1B has been studied as a carrier to target specific cancer cell types and deliver drugs efficiently

(El Alaoui et al., 2007; Geyer et al., 2016; Rosato et al., 2022). By the lectin-peptide fusion, we hypothesized that Stx1B would selectively target Gb3<sup>+</sup> tumor cells while RDP215 would kill them. As such, we expected the bispecific fusion product to be efficient at lower doses than RDP215 alone. If successful, our proof-of-concept study could expand the role of RDP215 in selective cancer killing because it might be fused to carriers that are selective for a variety of tumor cells.

The stability of peptides as single-agent drugs is a principal concern for use in peptide-based therapeutics (Böttger et al., 2017; Vlieghe et al., 2010). A study by Maxian et al. observed that RDP215 had a short half-life in 2% and 10% human serum in phosphate-buffered saline and postulated that it was the result of proteolysis by peptidases and proteinases (Maxian et al., 2021). Another study by Baggio and colleagues reported that linking peptides to larger proteins like human serum albumin reduced the renal clearance and extended the half-life (Baggio et al., 2008). The half-life of Shiga toxins in blood was estimated earlier to be around 4 days (Brigotti et al., 2006). In this regard, the lectin-peptide fusion may be stable in vivo, yet future studies will have to assess their half-life and stability (Conrady et al., 2010).

The main shortcoming of genetic fusions is that they connect polypeptides in a linear fashion. They do not allow us to join peptides or proteins to non-proteinaceous biomolecules like nucleic acids, lipids, or small molecules nor are branched conjugates possible. Chemical ligation on protein level allows the linear as well as branched conjugation of peptides to non-proteinaceous biomolecules. However, a lack of reactive canonical amino acids like lysine, tyrosine, or cysteine in a peptide impedes chemical conjugations at a selected position. On the other hand, more than one lysine, tyrosine, or cysteine might lead to conjugations at multiple sites or yield heterogenous products (Boutureira & Bernardes, 2015). Highly specific, regioselective, and rapid bioorthogonal conjugation reactions, such as the copper-catalyzed or strain-promoted cycloaddition of azides with alkynes (“click chemistry”) are an excellent alternative for the site-specific conjugation of peptides to proteins as well as to non-proteinaceous biomolecules (Zhang & Zhang, 2013). However, compatible reactive handles on both the conjugation partners are crucial to perform click reactions. In our recent work, we successfully installed a reactive azide group via N<sup>ε</sup>-((2-azidoethoxy)carbonyl)-L-lysine (AzK) in the lectin Stx1B and the T cell-specific single-chain variable fragment OKT3 in *Escherichia coli* (Rosato et al., 2022). Later, the proteins were conjugated using click reactions to produce a lectin body which was effective in cross-linking T cells with tumor cells and induced T cell-specific killing of the latter.

By and large, most peptides are synthesized by Fmoc solid-phase peptide synthesis (SPPS) which was also the

case with RDP215 (amino acid sequence: FWRIRRRPR-RIRIRWF, C-terminally amidated) (Behrendt et al., 2016; Riedl et al., 2014). Installing an nCAA into the peptide during Fmoc SPPS is an expensive method due to the requirement of Fmoc-protected nCAA derivatives. Therefore, our second aim was to optimize the recombinant production of rRDP215 (r, recombinant; amino acid sequence: AFWRIRRRPRRIRIRWFENLYFQ) and its AzK variant rRDP215 20AzK (amino acid sequence: AFWRIRRRPRRIRIRWF(AzK)ENLYFQ with AzK inserted at position 20) in *E. coli* as glutathione S-transferase (GST) fusion proteins. The fusion proteins contained a protease cleavage site to release the recombinant peptides. Finally, the cleaved and purified wildtype peptide rRDP215 was tested for functionality by cytotoxicity assays on glioblastoma LN-229 cells. The rRDP215 20AzK was labeled with a fluorophore to confirm the accessibility of AzK and further tested to bind HeLa cells by fluorescence assays. The clickable rRDP215 20AzK is “ready-to-conjugate” with proteins, peptides, nucleic acids, or small (drug) molecules to develop new tools for targeted cancer therapy and imaging.

## 2 | RESULTS

### 2.1 | Purification and characterization of lectin-peptide fusion proteins

The recombinant lectin-peptide fusion proteins were produced in *E. coli* and purified by Gb3-affinity chromatography. The hexhistidine tag on the C-terminus of the lectin-peptide fusions was inaccessible for IMAC purification (data not shown), and so we chose to purify by using Gb3 affinity matrix. The preparation of the matrix is presented as a scheme in Figure 1a, for details refer to the Additional file 1: Supplementary Methods. The RDP215 sequence was fused to the N- (RDP215-Stx1B) or C-terminus (Stx1B-RDP215) of the Stx1B. We spaced Stx1B and RDP215 with a short flexible GGGGS linker with small and polar amino acids glycine and serine to provide flexibility and solubility. The affinity-purified fusion proteins RDP215-Stx1B and Stx1B-RDP215 with a calculated molecular mass of ~12 kDa each, apparently occurred as trimers when separated on 4%–12% SDS-gels (Figure 1b,c). The protein titers per liter of culture were ~1 mg and ~1.4 mg for RDP215-Stx1B and Stx1B-RDP215, respectively. Mass spectrometry analysis of in-gel protein digests confirmed the identity of RDP215-Stx1B and Stx1B-RDP215. Peptide coverage from the protein mass analysis is given in Additional File 1: Figure S1 and Additional File 2: Table S1. The intact mass spectrometry was performed to identify the conformations of lectin-peptide fusion proteins but failed to generate data due to oligomerization (data not shown).

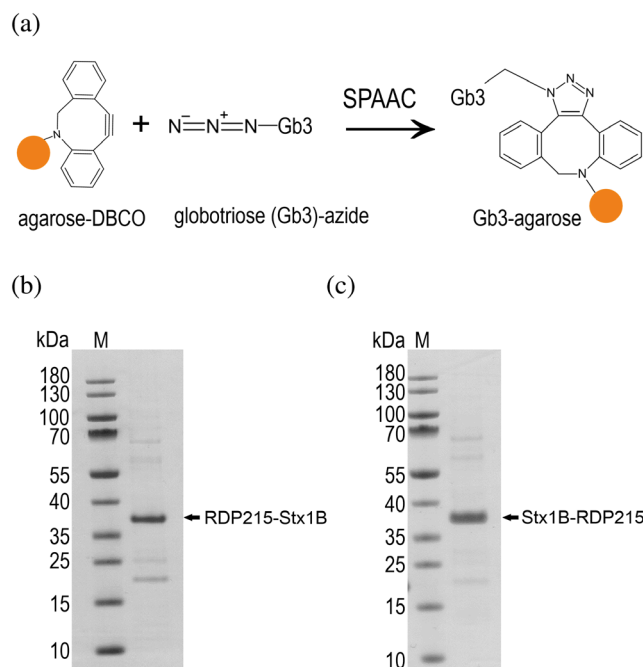


**FIGURE 1** Affinity purification of peptide-lectin fusion proteins using Gb3-functionalized agarose. (a) Schematic depiction of Gb3-agarose affinity matrix preparation by strain-promoted azide-alkyne cycloaddition of a dibenzocyclooctyne-functionalized matrix and Gb3-azide. SPAAC, strain-promoted alkyne-azide cycloaddition; Lane M, molecular weight markers in kDa; black arrows indicate protein bands of interest.

## 2.2 | The RDP215-Stx1B fusion construct selectively kills Gb3-expressing tumor cells

We hypothesized that the lectin-peptide fusions were selective for Gb3+ tumor cells and killed these cells better than RDP215 alone. To test the selective killing of Gb3+ tumor cells by lectin-peptide fusions using viability assays, we first selected appropriate cell lines with and without abundant Gb3. We assessed the presence/absence of Gb3 expression in the in-house cell lines HeLa and LN-229 by fluorescence-based cell binding assay using Stx1B-Cy3. The fluorescence microscopy images revealed selective binding of Stx1B-Cy3 to HeLa and not LN-229 cells indicating only HeLa cells expressed the Gb3 biomarker (Figure 2a).

The cytotoxic activity of RDP215 alone on HeLa cells was assessed for the first time in this study to compare it with the efficiency of the lectin-peptide fusions. Indeed, HeLa cells showed a peptide concentration-dependent decrease in their viability. Only ~20% viable cells persisted at the highest concentration of RDP215 tested in the assay (40  $\mu$ M; Additional file 1: Figure S2a). No significant effect on viability was observed at 5 or 10  $\mu$ M RDP215 (Additional file 1: Figure S2a). Earlier studies had confirmed the cytotoxicity of RDP215 toward LN-229 cells ( $LC_{50}$  8 h =  $1.7 \pm 0.1$   $\mu$ M) (Maxian et al., 2021).

Finally, the lectin-peptide fusion constructs RDP215-Stx1B and Stx1B-RDP215 were tested for selective targeting and killing of Gb3+ cancer cells by calcein

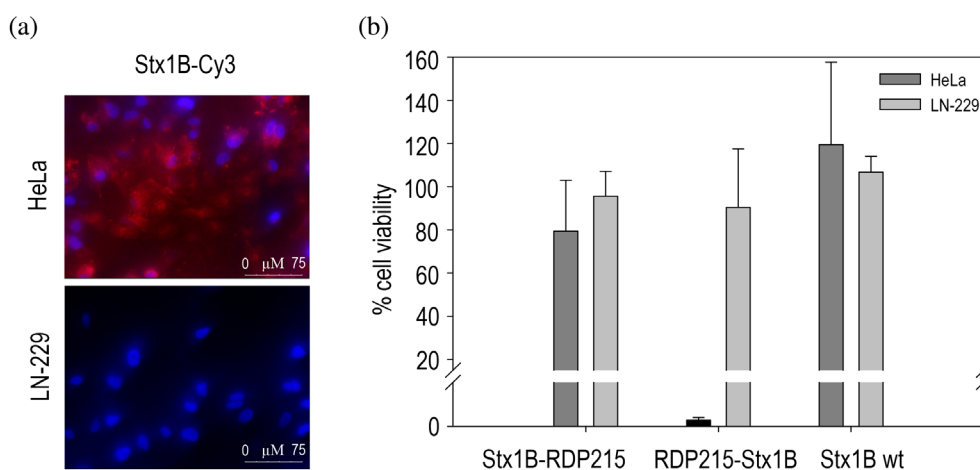


**FIGURE 2** Tumor cell binding of peptide-lectin fusion proteins and viability analysis. (a) Lectin Stx1B selectively detected Gb3 overexpressing tumor cells. We treated HeLa (upper panel) and LN-229 cells (lower panel) with 10  $\mu$ M of Stx1B-Cy3 and assessed the interaction by fluorescence microscopy. (b) RDP215-Stx1B killed Gb3-positive tumor cells selectively and effectively. We analyzed the cell viability with the calcein AM assay as described in the Section 5. Histograms represent percentage of viable HeLa and LN-229 cells after treatment for 24 h with 10  $\mu$ M each of the proteins Stx1B-RDP215 and RDP215-Stx1B. Cells were treated with Stx1B wt, 10  $\mu$ M as a negative control. The data represent the mean of four or more individual experiments, and the error bars denote the standard deviation. Slanted right axis-break is from 2% to 15%.

AM assay. The cell-permeant dye calcein AM (Thermo Fisher Scientific) undergoes acetoxymethyl ester hydrolysis by intracellular esterases in live cells to produce green-fluorescent calcein while dead cells are non-fluorescent. Neither RDP215-Stx1B nor Stx1B-RDP215 showed any significant decline in viability of HeLa or LN-229 cells at the peptide concentration of 5  $\mu$ M (Additional file 1: Figure S2b). However, less than 1% viable HeLa cells were observed upon treatment with higher concentrations as 10  $\mu$ M RDP215-Stx1B while LN-229 cells were mainly unaffected (Figure 2b). The results indicate that Stx1B in RDP215-Stx1B dominates the selectivity to target Gb3 and subdues the interaction of RDP215 with PS. At 10  $\mu$ M RDP215-Stx1B effectively killed >99% HeLa (Figure 2b) cells compared to low cytotoxicity of <20% observed at 10  $\mu$ M of RDP215 alone (Additional file 1: Figure S2a). At the maximum tested concentration of 40  $\mu$ M, RDP215 alone showed ~80% killing of HeLa cells (Additional file 1: Figure S2a). On the other hand, both HeLa and LN-229 cells were not sensitive to Stx1B-RDP215 (Figure 2b). These results suggest that Stx1B-RDP215 was not functional. As a negative control, we treated LN-229 cells with lectin-peptide fusions and they showed no sensitivity toward RDP215 in the fusions (Figure 2b). Treatment of HeLa and LN-229 cells with Stx1B wt as another control showed no cytotoxicity (Figure 2b). To conclude, only the RDP215-Stx1B lectin-peptide fusion showed efficient activity at lower concentration compared to the peptide alone. We achieved Gb3+ selectivity in RDP215-Stx1B and greatly minimized the drug concentration compared to RDP215 alone.

### 2.3 | Peptides rRDP215 and rRDP215 20AzK are successfully produced in *E. coli*

The greatly enhanced activity of a lectin-peptide fusion encouraged us to produce rRDP215 and rRDP215 20AzK in *E. coli*. The latter will have applications in bioconjugations as a “ready-to-conjugate” anticancer peptide. To begin with, we optimized the expression of rRDP215 in the cytoplasm of *E. coli*. The vectors pT7x33-GST-TEV-rRDP215-6xH and pT7x33-rRDP215-TEV-GST-6xH were designed with a GST-tag fusion at the N- and C- termini of rRDP215, respectively. Anti-His immunoblot analysis of the soluble and insoluble fractions for GST-rRDP215 and rRDP215-GST showed expression of the latter in both soluble and insoluble fractions (Figure 3a). In contrast, the protein GST-rRDP215 was not detected in either the soluble or insoluble fractions. Expression levels of rRDP215-GST ( $MW_{\text{calc}} \sim 30$  kDa) increased with an increase in the induction time from 0 to 4 h in both soluble and insoluble fractions. The recombinant fusion

proteins did not appear in the uninduced samples (Figure 3a, lanes 0 h) as expected. In the insoluble fractions of rRDP215-GST, a signal at the size of ~60 kDa suggests an rRDP215-GST dimer (Figure 3a, lanes 2 h and 4 h, insoluble fractions). However, an unspecific band appeared at ~40 kDa in all the samples including the uninduced ones, which suggests the accidental detection of an *E. coli* host protein. The full-length soluble rRDP215-GST was purified by immobilized glutathione affinity chromatography and analyzed using SDS-PAGE (Figure 3b). The protein titer of the soluble rRDP215-GST produced in the cytoplasm of *E. coli* was 6 mg per liter of culture.

The incorporation of AzK into the fusion protein rRDP215-GST 20AzK was achieved in *E. coli* using the expression construct pT7x33-rRDP215 20 am-TEV-GST-6xH as described in the materials and methods section. The titer of the purified soluble protein rRDP215-GST 20AzK was 6 mg per liter of culture which was comparable to the yields of wildtype protein rRDP215-GST. Both the peptides rRDP215 and rRDP215 20AzK as GST fusions were produced in the cytoplasm of *E. coli*. No target protein was produced in the absence of AzK (data not shown).

### 2.4 | SPAAC reaction aids in tracking efficiency of TEV protease

The GST-fused peptides produced in *E. coli* were subjected to TEV digestion to remove the GST-tag and release the peptides. However, we experienced staining issues of the cleaved peptides when analyzed on SDS gels. The recombinant peptides were not well stained with Coomassie and if stained, the bands disappeared in less than 1 h during de-staining. Therefore, we made use of the SPAAC reaction to label rRDP215 20AzK with a fluorophore to be able to track the peptide and the efficiency of TEV cleavage. The construct to produce rRDP215-GST 20AzK carried a TEV protease cleavage site between the N-terminal AzK-labeled peptide and the C-terminal GST-tag as detailed in the Additional file 1: Figure S3f. The full-length protein rRDP215-GST 20AzK was cleaved using TEV protease. The protein was labeled with a DBCO-Cy3 fluorophore via SPAAC before and after TEV cleavage. The reaction mixtures were separated on tricine-SDS-gels and stained with Coomassie stain (Figure 4a,c). We also monitored the fluorescence under UV illumination before Coomassie staining (Figure 4b,d). Visible fluorescent bands of rRDP215-GST-Cy3 ( $MW_{\text{calc}} \sim 30$  kDa) and rRDP215-GST-Cy3 dimer ( $MW_{\text{calc}} \sim 60$  kDa) indicate successful incorporation of AzK and labeling of the protein before cleavage (Figure 4b, lane -TEV). After TEV cleavage, the peptide rRDP215-Cy3

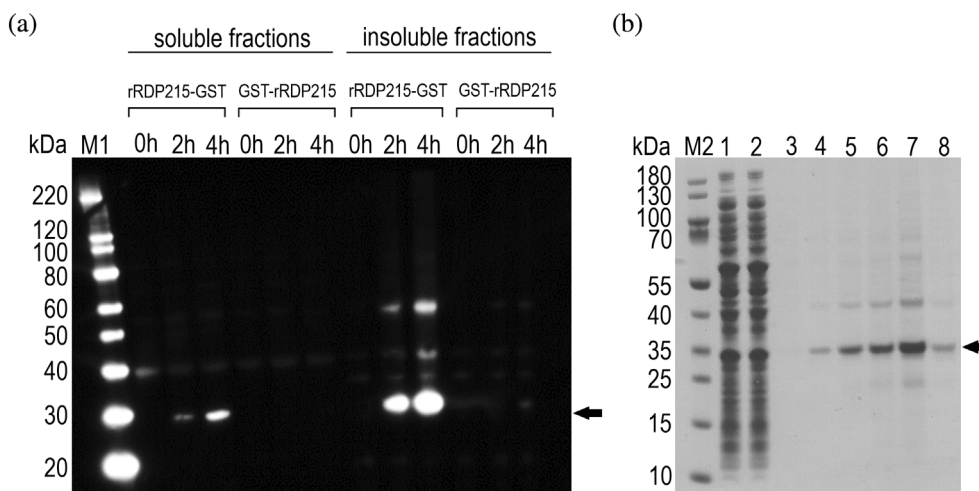


**FIGURE 3** Production of rRDP215 as GST-fusion protein in *E. coli* and the purification. (a) Anti-his immunoblot analysis revealed expression of the rRDP215-GST fusion but not of the GST-rRDP215 fusion protein. The details of the fusion constructs are depicted in the Additional file 1: Figure S3d,e. Soluble and insoluble protein fractions before induction (0 h) and 2 and 4 h after induction of the gene expression with IPTG were separated on a 4%–12% SDS-gel. Proteins were transferred to a nitrocellulose membrane and were probed by mouse anti-6x-His tag monoclonal primary antibody and goat anti-mouse secondary antibody-HRP conjugate. The black arrow indicates rRDP215-GST ( $MW_{\text{calc}} \sim 30$  kDa); M1, MagicMark XP Western Protein Standard (Thermo Fisher Scientific). (b) Coomassie stained SDS-gel showing the purification of rRDP215-GST by immobilized glutathione affinity chromatography. M2, molecular mass standards in kDa; Lane 1, clarified lysate; lane 2, flow through after loading clarified lysate on a glutathione agarose column; lane 3, column wash with reduced L-glutathione; lanes 4–8, elution fractions.

( $MW_{\text{calc}} \sim 3.5$  kDa) and uncleaved full-length rRDP215-GST-Cy3 were detected as fluorescent bands (Figure 4d, lane +TEV). The GST-tag ( $MW_{\text{calc}} \sim 26$  kDa) after TEV protease cleavage was non-fluorescent and observed as a band below the full-length rRDP215-GST-Cy3 on the Coomassie-stained gel only (Figure 4c vs. d, lanes 2). As expected, the SPAAC aided in tracking the isolated peptide by fluorescence whereas Coomassie staining revealed only a very faint band on the tricine-SDS gel (Figure 4c, lane 2).

## 2.5 | rRDP215 and rRDP215 20AzK can be purified by size-exclusion chromatography

The wildtype peptide rRDP215 was cleaved by TEV protease as described for rRDP215 20 AzK. The tracking of rRDP215 was not possible as it lacks AzK. To purify the recombinant peptides after TEV cleavage of the GST-tag, we employed size-exclusion chromatography (SEC). Representative SEC chromatograms of the purification of the recombinant peptides rRDP215 and rRDP215 20AzK and the synthetic peptide RDP215 as a benchmark are given in the Additional file 1: Figure S4. The molecular weights observed for rRDP215 and rRDP215 20AzK were calculated using calibration standards of known size as shown

in the Additional file 2: Table S2 and Figure 5a. The pure fractions of rRDP215 20AzK from size-exclusion chromatography were labeled with DBCO-Cy3 via SPAAC click reaction to confirm AzK reactivity. The Coomassie-stained 10%–20% tricine-SDS-gel showed both the synthetic peptide RDP215 and the SEC-purified rRDP215 20AzK fractions (Figure 5b). Under UV light before Coomassie staining, only the recombinant rRDP215 20AzK labeled with the Cy3-fluorophore showed a fluorescent band while RDP215, which lacked AzK, did not (Figure 5c). We processed the peptides rRDP215 and rRDP215 20AzK for intact MS analysis, but it was unsuccessful due to the small size of the peptides, the repetitive amino-acid arginine, and insufficient amounts. The pure peptide yield was 0.5 mg per liter of culture for both rRDP215 and rRDP215 20AzK.

The yields of pure peptides from SEC varied with each run. To make the purification of the peptide more robust and to improve its yields, we switched to reversed-phase high-performance liquid chromatography (RP-HPLC). We optimized the RP-HPLC conditions using the synthetic peptide RDP215 as it was available in the required quantities. A representative chromatogram is presented in the Additional file 1: Figure S5a. The fractions collected from the peak (12 mL) were pooled, concentrated, and separated on a tricine-SDS-gel showing pure RDP215 (Additional file 1: Figure S5b).

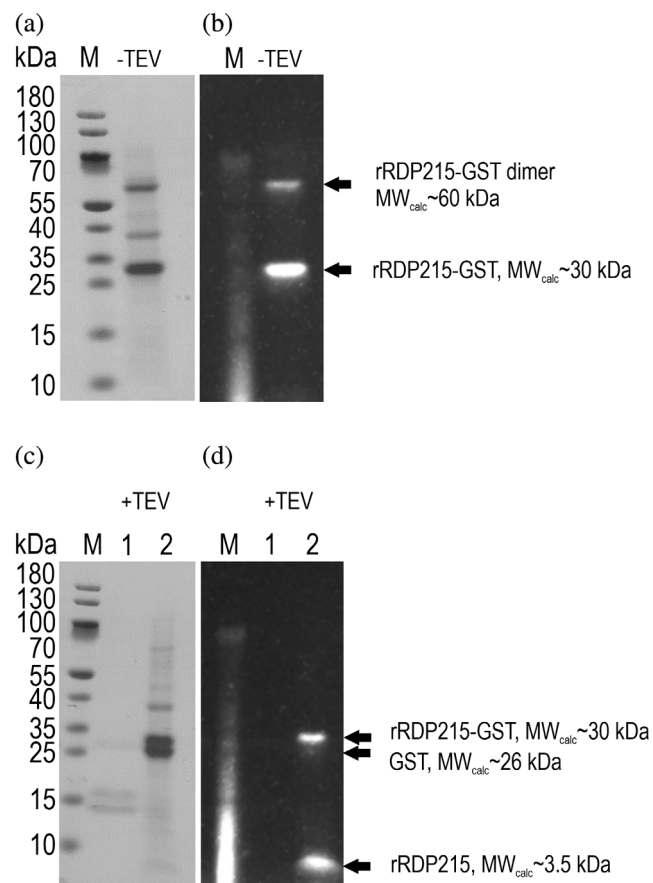


**FIGURE 4** SPAAC click reaction aids in tracking cleavage of GST-fusion tag. The purified full-length protein rRDP215-TEV-GST 20AzK ( $MW_{\text{calc}} \sim 30$  kDa) before (-TEV) and after (+TEV) cleaving by TEV protease was labeled with DBCO-Cy3 via SPAAC as described in the Additional file 1: Supplementary [Methods](#). Proteins were separated on 10-20% tricine-SDS gels. The proteins were stained with Coomassie protein staining (panels a and c) after visualizing them under UV irradiation at 305 nm (panels b and d). The control reaction contains TEV protease (TEV,  $\sim 26$  kDa) and DBCO-Cy3 only. M, molecular mass standards in kDa; lane 1, control (0.3  $\mu\text{g}$ ); lane 2, sample from +TEV cleavage reaction.

## 2.6 | rRDP215 and rRDP215 20AzK are functional

To assess the functionality of the SEC-purified peptides, rRDP215 that lacks AzK was tested for cytotoxicity on LN-229 cells and rRDP215 20AzK labeled with a fluorophore to bind HeLa cells. The amounts of the produced peptides were too low to perform analysis with both HeLa and LN-229 cells. Therefore, we chose to work with LN-229 in the cytotoxicity assay because these cells are very sensitive to the synthetic peptide RDP215 at low concentrations ( $LC_{50} = 1.7 \pm 0.1 \mu\text{M}$ ) (Maxian et al., 2021) compared to HeLa ( $LC_{50} = >20 \mu\text{M}$ , Figure S2a). The fluorophore-labeled peptide rRDP215-Cy3 was used for cell binding assays on HeLa cells.

Functionality of the recombinant peptide rRDP215 was confirmed by PI-cytotoxicity assay against LN-229 cells (Figure 6a) although the activity was halved compared to the synthetic peptide RDP215 (Maxian et al., 2021). The fluorophore-labeled recombinant peptide rRDP215-Cy3 bound HeLa cells via overexposed PS confirming that the binding of hLFcin-derived peptides to cancer cells was preserved in this bioconjugate. Treatment with DBCO-Cy3 alone did not show any fluorescence indicating no unspecific binding of the fluorophore (Figure 6b). Therefore, the peptides rRDP215 and rRDP215 20AzK produced in *E. coli* in the current study were functional. Our findings suggest that it can find application as a “clickable killing partner” for future bifunctional bioconjugates or as a tracker in cancer metastasis imaging.

## 2.7 | Recombinant rRDP215 shares a similar structure with synthetic RDP215

The structure, net charge, and hydrophobicity of a peptide are essential for its cytotoxicity toward tumor cells (Grissenberger et al., 2020; Riedl et al., 2014). We predicted these parameters for rRDP215 produced in *E. coli* in this study to compare them to the synthetic peptide RDP215. The structure prediction revealed a  $\beta$ -sheet conformation for RDP215 and rRDP215 (Additional file 1: Figure S6). The net charge was calculated to be +9 for RDP215 (FWRIRIRPRRIRIRWF), C-terminally amidated) and +7 for rRDP215 (AFWRIRIRPRRIRIRWFENLYFQ). Peptide hydrophobicity according to Wimley and White (Wimley & White, 1996) expressed as transfer free energy of peptides from water to POPC (1-palmitoyl-2-oleoyl-*sn*-glycero-3-phosphocholine) was  $-0.27$  kcal/mol for RDP215 and  $0.29$  kcal/mol for rRDP215. The structural and biophysical similarities from our prediction correlate to the functional activity against tumor cells, that is, cytotoxicity as detailed in the previous section.

## 3 | DISCUSSION

In this study, we fine-tuned the selectivity of the hLFcin-derived peptide RDP215 toward a specific cancer cell type by fusing it to the lectin Stx1B on the gene level. Furthermore, we produced a clickable recombinant peptide rRDP215 20AzK and covalently conjugated it to a fluorophore for application, for example, in imaging cancer cells. The peptide rRDP215 20AzK is a “ready-to-conjugate” molecule for future applications in targeted drug delivery and imaging tumor metastasis.

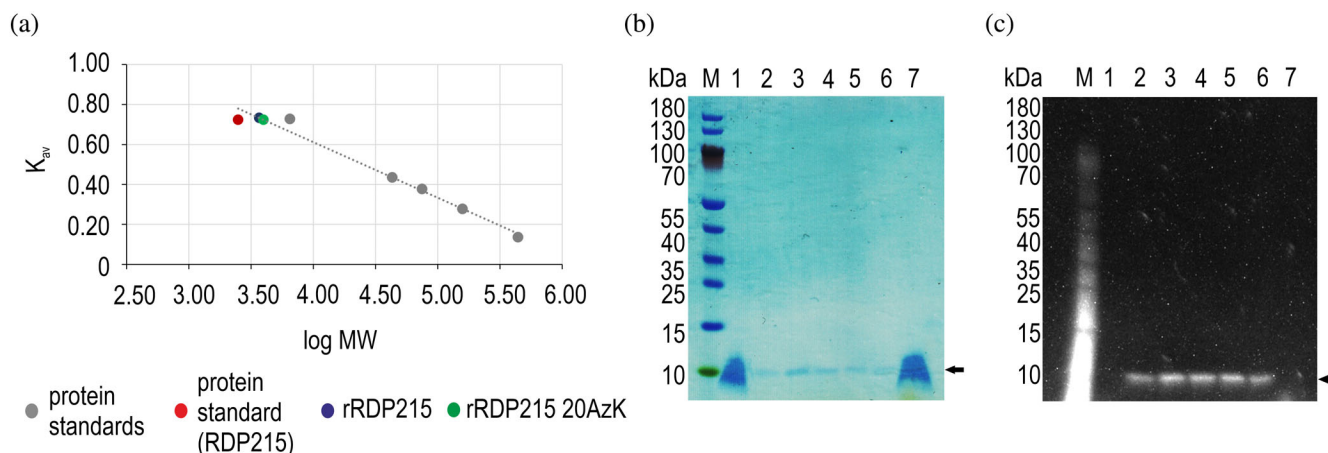


**FIGURE 5** Molecular size analysis of rRDP215 20AzK and fluorophore labeling. (a) The calculated molecular weights of rRDP215 (3.6 kDa) and rRDP215 20 AzK (3.9 kDa) in comparison to RDP215 (2.5 kDa). For mass analysis details, refer to Additional file 2: Table S2. Log MW, logarithm of molecular weight;  $K_{av}$ , gel-phase distribution constant. Purified rRDP215 20AzK was labeled with the fluorophore DBCO-Cy3 by SPAAC as described in the Additional file 1: Supplementary methods. As a negative control, synthetic peptide RDP215 (5  $\mu$ g) that lacks AzK was incubated with DBCO-Cy3. Proteins after SPAAC were separated on a 10%–20% tricine-SDS gel: (b) Coomassie stained gel; (c) gel irradiated with UV before Coomassie protein staining. M, molecular mass standards in kDa. Lanes 1 and 7, synthetic peptide RDP215 (2  $\mu$ g); lanes 2–6, purified fractions of rRDP215 20AzK from SEC.

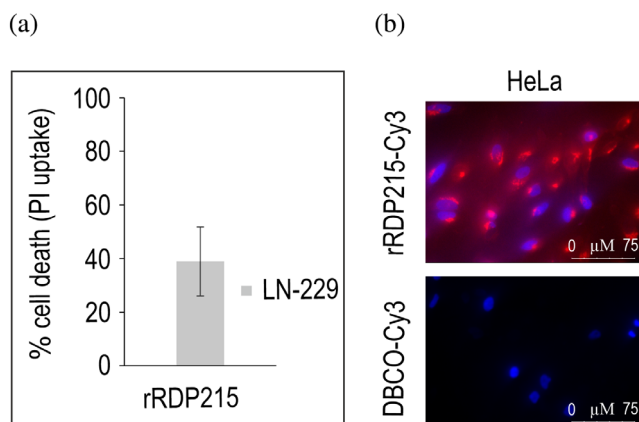


**FIGURE 6** Cytotoxicity and cancer cell binding ability of the recombinantly produced peptides rRDP215 and rRDP215 20AzK, respectively. (a) Propidium iodide (PI) uptake was measured 8 h post treatment with rRDP215 in glioblastoma cell line LN-229. PI-uptake was used as an indicator of cell death. The bar chart represents percentage cell death calculated from the mean values of three individual experiments. The error bar denotes standard deviation. (b) Upper panel shows representative fluorescence micrographs of HeLa cells labeled with rRDP215-Cy3 (10  $\mu$ M) produced by SPAAC of rRDP215 20AzK with DBCO-Cy3. The lower panel shows the negative control treated with DBCO-Cy3 (100  $\mu$ M). Nuclear staining with DAPI is shown in blue.

Genetic constructs were made that fused RDP215 to the N- or C- terminus of Stx1B. The fusion proteins were produced in the cytoplasm of *E. coli* and purified by Gb3 affinity chromatography. Purification of Shiga toxin lectins using affinity matrices with Gb3 adsorbed on celite

or octyl sepharose, or chemically attached Gb3 was accomplished in earlier studies (Boulanger et al., 1994; Nakajima et al., 2001; Pozsgay et al., 1996). The celite adsorption method lacks space between the matrix and the Gb3 oligosaccharide which reduces the flexibility of Gb3. In this study, Gb3 was covalently conjugated to agarose functionalized with DBCO on short linker molecules, using SPAAC click reaction. The Gb3 affinity purified fusion proteins RDP215-Stx1B and Stx1B-RDP215 migrated at an apparent molecular weight that was three times higher (36 kDa; Figure 1b) than calculated for the monomers (12 kDa). Nevertheless, peptide mapping confirmed the identity of both proteins (Additional file 2: Table S1). The fusion proteins apparently formed SDS-resistant trimers. Hydrophobic regions on each of the fusion partners might be the basis for SDS-resistant oligomerization as reported previously for GroES and ubiquitin fused to A $\beta$ 42 peptide, which were produced in *E. coli* (Ngo & Guo, 2011; Ochiishi et al., 2016). Dolezal et al. observed the formation of dimers, trimers, tetramers, and multimers with shortening of the linker between variable light and heavy chains of anti-neuraminidase antibody single-chain variable fragment (Dolezal et al., 2000). Adjusting the length of the short peptide linker between the fusion partners might resolve the SDS-resistant trimers in our case.

Mass analysis of in-gel tryptic and chymotryptic digests of the fusion proteins did not cover the peptide RDP215 in full. This can be explained by 8 arginine, 3 isoleucine, 2 tryptophan, and 3 phenylalanine residues in the 25-amino acid peptide RDP215, which are all specific

substrates for trypsin and chymotrypsin. The peptides WFGGGSTPDCVTGK and GGGGSFWR clearly confirmed the identity and orientation of RDP215 in RDP215-Stx1B and Stx1B-RDP215, respectively (refer to Additional file 2: Table S1).

One of the two fusion proteins, RDP215-Stx1B was biologically highly active in selectively targeting and killing Gb3-positive cancer cells. HeLa cells were >99% sensitive to RDP215-Stx1B at 10  $\mu$ M whereas only ~20% of the cells were killed when treated with 10  $\mu$ M synthetic peptide RDP215. It took 40  $\mu$ M synthetic RDP215 to kill ~80% HeLa cells. This suggests that RDP215-Stx1B is five times more efficient in killing Gb3+ tumor cells than the synthetic peptide RDP215 alone at the same concentration. This demonstrates the receptor specificity of RDP215-Stx1B toward Gb3-expressing tumor cells. The control Stx1B wt did not affect the viability of HeLa nor LN-229 cells at the tested concentrations indicating Stx1B has no role in inducing cell death. LN-229 cells treated with RDP215-Stx1B showed no measurable decrease in viability, which correlates with the inability of Stx1B-Cy3 to bind to LN-229 cells that lack Gb3. Our results proved effective bispecificity of RDP215-Stx1B, where Stx1B bound Gb3+ HeLa cells and RDP215 induced cell death. By fusing Stx1B to RDP215, we have successfully expanded the selectivity of RDP215 from solely PS-positive to Gb3-positive tumor cells. The single-agent peptide drug RDP215 otherwise targets both HeLa (current study) and LN-229 cells via exposed PS (Maxian et al., 2021). Though RDP215 alone can induce cell death in HeLa cells, the concentration required was more than five times higher than RDP215-Stx1B to exert the highest cytotoxic effect as described above. Our results are in accordance with the study by El Alaoui and co-workers where cytotoxicity was observed in Gb3 expressing colorectal cell line HT29 treated with a prodrug STxB-SN38 (El Alaoui et al., 2007). SN38 is the active metabolite of irinotecan. The same study showed no or less cytotoxicity on PPMP (DL-threo-1-phenyl-2-palmitoylamino-3-morpholino-1-propanol, a chemical inhibitor of glucosylceramide synthesis) treated HT29 and CHO cells, which lack Gb3. A report by Geyer et al. showed a >100-fold increase in cytotoxicity towards a Gb3 expressing gastric carcinoma cell line when treated with STxB-SN38 compared to irinotecan alone (Geyer et al., 2016). In addition, negligible cytotoxicity was reported with Stx1B on CHO fibroblast cells and with RDP215 on human melanocytes, NHDF (Normal Human Dermal Fibroblasts), and NHEM (Normal Human Epidermal Melanocytes) cell lines at concentrations of 10–20  $\mu$ M (El Alaoui et al., 2007; Grissenberger et al., 2020; Maxian et al., 2021; Riedl et al., 2014). Therefore, the current study reports a novel fusion protein RDP215-Stx1B as an addition to the tools

to investigate and target Gb3-positive tumors like gastric carcinoma, colorectal adenocarcinoma, and breast carcinoma.

Our results also revealed that RDP215 fused to the C-terminus of Stx1B rendered the construct ineffective against cancer cells. This might be due to loss of function of the peptide RDP215 as Stx1B-RDP215 was purified by Gb3 affinity chromatography which suggests functional Stx1B. The loss of function can be attributed to structural disturbances. Again, different linkers and linker lengths between the fusion partners might alleviate potential structural disturbances. There are reports where an addition of a 12-amino acid helix-forming linker between interferon- $\alpha$ 2b fused on the C-terminus of human serum albumin increased anti-viral activity by 115% (Zhao et al., 2008). Site-specific conjugation of fusion partners on the protein level could be a prudent choice to avoid non-functional fusions like Stx1B-RDP215. Therefore, we produced recombinant peptide rRDP215 and incorporated the reactive nCAA, AzK into rRDP215 in *E. coli* for bioconjugations by site-specific click reactions.

Here, the N-terminal rRDP215 fused to GST was produced while no expression was observed with C-terminal rRDP215 fused to GST. It is not surprising as the efforts by Chen et al. and Skosyrev et al. to produce the antimicrobial peptides ABP-CM4 and sarcotoxin as fusions on the C-terminus of GST failed due to low expression and degradation during purification (Chen et al., 2008; Skosyrev et al., 2003). In the current study, the overexpressed rRDP215-GST occurred in the insoluble protein fraction more abundantly compared to soluble protein. As the protein titers were sufficient to carry out the experiments, we preferred to work with the soluble fractions to avoid tedious denaturation and refolding steps. Zorko and colleagues recombinantly produced and purified the hLFcin-derived and RDP215-related peptide PFWRIRIR (PFR) from inclusion bodies in *E. coli* (Zorko et al., 2009). The yield of pure PFR peptide (10 mg) per liter of culture was 20 times more than rRDP215 (0.5 mg) produced in this study. However, the isolation of pure peptide PFR from the full-length fusion protein was only 2% (10 mg from 550 mg per liter of culture) while it was 10% (0.5 mg from 5 mg per liter of culture) for rRDP215 in this study. Wingfield stated that >50% recovery can be expected with soluble proteins and only 5%–20% with insoluble proteins due to considerable loss during the denaturation and folding cycles (Wingfield, 2015). The recovery of peptides from inclusion bodies indeed decreases the production yield and increases the production costs (Sadeghian-Rizi et al., 2019). Hence for future applications, the production of recombinant peptide rRDP215-GST can be

performed in fed-batch bioreactor cultures to increase the biomass which in turn may increase the yield of soluble protein.

Like the wildtype, the azide variant rRDP215-GST 20AzK was produced in soluble form and the GST-tag was cleaved by TEV protease to isolate the rRDP215 20AzK peptide. The protein titers were similar to wildtype rRDP215-GST indicating high efficiency of the AzK incorporation by the orthogonal wildtype pyrrolysyl-tRNA synthetase/tRNA<sub>CUA</sub><sup>Pyl</sup> pair from *Methanosarcina mazei*. It was reported that some peptides do not stain with Coomassie and need increased loading volumes during SDS-PAGE to visualize (Sarfo et al., 2003). Therefore, we tracked the isolation of rRDP215 peptide by labeling it with the fluorophore Cy3 via SPAAC. The labeling enabled the detection of fluorescent rRDP215-GST before TEV cleavage as well as rRDP215 peptide after TEV cleavage. The strategy also allowed tracking of the TEV cleavage efficiency, which was incomplete yet sufficient for the subsequent experiments after incubation for 6 h at 4°C. We observed an rRDP215-GST dimer, which was not surprising as GST has the ability to form homodimers (Ji et al., 1992; Parker et al., 1990). The isolated peptides were purified by SEC and the molecular weights were analyzed by tricine-SDS-PAGE. We devised an alternate RP-HPLC method for polishing the recombinant peptide, which we optimized with the synthetic peptide. Initial experiments with the recombinant peptide were promising (data not shown), however further analysis will have to confirm whether this procedure improves the yields of pure recombinant rRDP215. The rRDP215 showed only half the killing efficiency in comparison to the synthetic peptide (Figure 6a) (Maxian et al., 2021). This might have different reasons: (1) the recombinant peptide might have impurities that were below the detection limit of our analysis or (2) could originate with the subtle differences in structure and physicochemical properties of the two peptide species. Further analyses of a cleaner, for example, RP-HPLC polished rRDP215 are required to explore its activity in more detail. The AzK incorporation in rRDP215 20 AzK was confirmed by Cy3-labelling via SPAAC. The biorthogonal click reaction was specific to the azide in rRDP215 20AzK but did not occur with the synthetic peptide RDP215, which we used as the control. The cytotoxicity of recombinant rRDP215 and the cancer cell binding ability of recombinant rRDP215-Cy3 evidently qualifies the molecule for bioconjugations, for example, with tumor-targeting antibody fragments (Cortez-Retamozo et al., 2002), lectins (Kurahde et al., 2022), nanoparticles (Vaughan et al., 2020) and small molecules (Liu et al., 2022) to generate new tools for cancer-cell-selective therapy and imaging of cancer cells or cancer metastasis.

## 4 | CONCLUSIONS

Taken together, the collective findings of the current study demonstrate the efficacy of bispecific lectin-peptide fusions in targeted cancer drug delivery and killing. The human lactoferricin-derived peptide R-DIM-P-LF11-215 (RDP215) genetically fused to the N-terminus of the lectin Stx1B selectively targeted Gb3-positive tumor cells and delivered the cytotoxic peptide efficiently at lower doses compared to the peptide alone. Hence the current study finds RDP215-Stx1B as a potential fusion protein for future studies on cancer-cell-selective killing applications. Further, the peptide rRDP215 was expressed in *E. coli* for the first time as a full-length GST fusion, the tag was cleaved, and the recombinant peptide was purified at reasonable titers. For future applications in conjugating rRDP215 to proteinaceous and/or non-proteinaceous biomolecules for cancer therapy, the reactive ncAA AzK was incorporated to produce a “clickable” rRDP215 20AzK. The functionality of AzK in rRDP215 20AzK was confirmed by labeling with the fluorophore cyanin 3. Therefore, the present study introduces “clickable” rRDP215 20AzK for future applications in imaging cancers and cancer metastasis by bioorthogonal conjugation with fluorophores or radionuclides. The clickable rRDP215 20AzK could also allow for site-specific biorthogonal conjugation of cytotoxic drugs. Future in vivo studies using the RDP215-Stx1B fusion can provide more information on the selectivity, safety, and efficacy of this new anti-cancer tool.

## 5 | MATERIALS AND METHODS

### 5.1 | Construction of expression plasmids

Genes encoding target proteins were ordered as synthetic gBlock gene fragments from Integrated DNA Technologies, Inc., IA, and are listed in the Additional file 2: Table S3. Restriction enzymes (FastDigest) were purchased from Thermo Fisher Scientific (Waltham, MA). The in-house target vector pT7x33 (Figure S3a) harbors genes to encode the orthogonal PylRS/tRNA<sub>CUA</sub><sup>Pyl</sup> pair from *Methanosarcina mazei* for AzK incorporation. The vector pT7x33 differs from pT7x32 (Pasupuleti et al., 2023) in the orientation of the *lacI* gene. Target vector pT7x33 was used to subclone the genes. All the constructs have a C-terminal hexahistidine tag. Two constructs were designed for the lectin-peptide fusion proteins RDP215-Stx1B and Stx1B-RDP215, one with RDP215 fused to the N-terminus and the other to the C-terminus of Stx1B. The fusion partners RDP215

and Stx1B were linked by the short linker GGGGS. The gBlocks pBP2848 and pBP2849 were restriction subcloned into pT7x33 using NdeI/NotI restriction enzymes to construct pT7x33-RDP215-Stx1B-6xH and pT7x33-Stx1B-RDP215-6xH, respectively (Additional file 1: Figure S3b,c). To produce the recombinant peptide as a GST-fusion protein, two constructs were designed. The gBlocks pBP2846 and pBP2847 were subcloned into pT7x33 to produce pT7x33-rRDP215-TEV-GST-6xH and pT7x33-GST-TEV-rRDP215-6xH, respectively (Additional file 1: Figure S3d,e). The plasmid to incorporate AzK into rRDP215 was constructed by subcloning the gBlock pBP2860 with an amber codon (TAG) corresponding to position 20 in rRDP215-GST into pT7x33 to generate pT7x33-rRDP215 20 am-TEV-GST-6xH (Additional file 1: Figure S3f). The position counting started with methionine at position 1 although the N-terminal methionine was most probably excised. Amino acid sequences of all the proteins used in this study and the chemical structure of AzK are given in Additional file 2: Table S4. Chemically competent *E. coli* BL21(DE3) cells (Merck KGaA, Darmstadt, Germany) were transformed with the sequence-verified plasmids and were stored in 30% glycerol at  $-80^{\circ}\text{C}$ .

## 5.2 | Protein production and purification

Recombinant protein expression and site-specific incorporation of AzK into proteins via genetic code expansion in *E. coli* was carried out as described previously (Rosato et al., 2022). Briefly, gene expression was induced with 0.3 mM IPTG at  $20^{\circ}\text{C}$  for 16–19 h, and 5 mM AzK were added at induction. The cell pellets (from 1-liter culture) harvested after expression of the lectin-peptide fusion proteins RDP215-Stx1B and Stx1B-RDP215 were resuspended in 75 mL of Tris buffer, pH 8.0. Cells were lysed using sonication (Branson Sonifier 250, Emerson Electric, St. Louis, MO) for 3 min on ice and centrifuged at 21000 rpm (JA-25.50 rotor, Beckman Coulter Life Sciences, IN) for 30 min. The supernatant (clarified cell lysate) was loaded onto the Gb3-agarose column for the Stx1B in the fusion proteins to bind Gb3 and the flow-through was collected. The non-specifically bound proteins were washed off with 25 mL Tris buffer, pH 8.0. Elution buffer (4 M  $\text{MgCl}_2$  in Tris buffer, pH 8.0) was used to elute the column-bound proteins in fractions of 0.75 mL. The protein concentration was determined by measuring the absorbance at 280 nm using a spectrophotometer (Thermo Scientific Inc., Rockford, IL). Fractions with the highest protein concentration were pooled and the buffer was exchanged to PBS by dialysis using a slide-A lyzer dialysis cassette with 3.5 kDa MWCO (Thermo Fisher Scientific). The GST fusion proteins

rRDP215-GST, GST-rRDP215, and rRDP215-GST 20AzK were purified in a similar way except that PBS was used to resuspend the cell pellet and PureCube glutathione agarose matrix (Cube Biotech GmbH, Monheim am Rhein, Germany) to capture the proteins. Wash and elution steps were performed with PBS and 50 mM reduced L-glutathione (Cube Biotech GmbH) in PBS, respectively. The lectins Stx1B K9AzK and Stx1B wildtype (Stx1B wt) were produced and purified according to the established method (Rosato et al., 2022).

## 5.3 | Cell lines and culture

The HeLa (ACC 57) cell line purchased from DSMZ GmbH (German Collection of Microorganisms and Cell Cultures, Leibniz Institute, Braunschweig, Germany) was cultured in Minimum Essential Media with GlutaMAX (Gibco, Thermo Fisher Scientific) supplemented with 10% FBS (fetal bovine serum, Gibco) and 0.1 mM non-essential amino acids (NEAA, Gibco). Glioblastoma cell line LN-229 from ATCC (American Type Culture Collection, Manassas, VA) was cultured in Dulbecco's Modified Eagle Medium DMEM with GlutaMAX (Gibco, Thermo Fisher Scientific) supplemented with 10% FBS. All cells were cultivated at  $37^{\circ}\text{C}$  in a humidified incubator with 5%  $\text{CO}_2$ . At 90% confluence, cells were detached with accutase (Gibco, Thermo Fisher Scientific) and were passaged.

## 5.4 | Calcein AM cell viability assay

Cells were seeded on 96-well transparent bottom plates at a concentration of  $1 \times 10^5$  cells/well in 100  $\mu\text{L}$  respective growth media. Cells were treated with 5  $\mu\text{M}$  and 10  $\mu\text{M}$  final concentrations of Stx1B wt, RDP215-Stx1B, and Stx1B-RDP215 and incubated for 24 h in 5%  $\text{CO}_2$  at  $37^{\circ}\text{C}$ . For RDP215, cells were incubated with 5, 10, 20, and 40  $\mu\text{M}$  final concentrations. Controls contained cells with culture media only. A 50  $\mu\text{M}$  working solution was prepared from 1 mM freshly prepared stock solution with dimethyl sulfoxide. Calcein AM (2  $\mu\text{L}$  from working solution) was added to each well after 24 h of treatment with the respective peptides and proteins. Fluorescence was recorded using GloMax<sup>®</sup> Explorer Multimode Microplate Reader (Promega, Madison, WI). Viable cell percentage was calculated by the following equation:

$$\% \text{ cell viability} = \frac{100 \times (P_x - P_{100})}{(P_0 - P_{100})}$$

where  $P_0$  is the arbitrary fluorescence units (AFU) from cells in media alone,  $P_x$  is AFU from cells treated with peptides and proteins, and  $P_{100}$  is AFU from cells after

treating with 2% Triton-X-100. Each experiment has duplicates and was repeated at least thrice.

## AUTHOR CONTRIBUTIONS

The authors confirm contribution to the paper as follows: *Conceptualization*: Rajeev Pasupuleti; *Writing-original draft*: Rajeev Pasupuleti; *Data curation*: Rajeev Pasupuleti and Sabrina Riedl; *Formal analysis*: Rajeev Pasupuleti and Sabrina Riedl; *Investigation*: Rajeev Pasupuleti, Sabrina Riedl, Marianna Karava, Dagmar Zweytick, Laia Saltor Núñez, Vajinder Kumar; *Project administration*: Birgit Wiltschi and Dagmar Zweytick; *Supervision*: Birgit Wiltschi, Dagmar Zweytick, Sabrina Riedl, W. Bruce Turnbull; *Review & editing*: Birgit Wiltschi, Dagmar Zweytick, W. Bruce Turnbull and Robert Kourist. All authors read and approved the final manuscript.

## ACKNOWLEDGMENTS

We thank Dr. Felix Tobola for providing TEV protease. Dr. Clemens Grünwald-Gruber and Rudolf Figl at the BOKU core facility mass spectrometry, Vienna, are acknowledged for assistance with protein mass analysis.

## FUNDING INFORMATION

This project has received funding from the European Union's Horizon 2020 research and innovation program under the Marie Skłodowska-Curie grant agreement No. 814029 and 746421. The COMET center: acib: Next Generation Bioproduction is funded by BMK, BMDW, SFG, Standortagentur Tirol, Government of Lower Austria und Vienna Business Agency in the framework of COMET—Competence Centers for Excellent Technologies. The COMET-Funding Program is managed by the Austrian Research Promotion Agency FFG (grant number 872161). Work was further funded by the Austrian Research Promotion Agency (FFG; Grant no. 855671). Open access funding provided by University of Natural Resources and Life Sciences Vienna (BOKU).

## CONFLICT OF INTEREST STATEMENT

The authors declare that they have no competing interests.

## DATA AVAILABILITY STATEMENT

All data generated or analyzed during this study are included in this published article [and its supplementary information files].

## ORCID

Vajinder Kumar  <https://orcid.org/0000-0002-8825-3517>  
Birgit Wiltschi  <https://orcid.org/0000-0001-5230-0951>

## REFERENCES

- Baggio LL, Huang Q, Cao X, Drucker DJ. An albumin-exendin-4 conjugate engages central and peripheral circuits regulating murine energy and glucose homeostasis. *Gastroenterology*. 2008; 134(4):1137–47. <https://doi.org/10.1053/j.gastro.2008.01.017>
- Barragán-Cárdenas AC, Insuasty-Cepeda DS, Cárdenas-Martínez KJ, López-Meza J, Ochoa-Zarzosa A, Umaña-Pérez A, et al. LfcinB-derived peptides: specific and punctual change of an amino acid in monomeric and dimeric sequences increase selective cytotoxicity in colon cancer cell lines. *Arab J Chem*. 2022;15(8):103998. <https://doi.org/10.1016/j.arabjc.2022.103998>
- Baudino TA. Targeted cancer therapy: the next generation of cancer treatment. *Curr Drug Discov Technol*. 2015;12(1):3–20. <https://doi.org/10.2174/1570163812666150602144310>
- Behrendt R, White P, Offer J. Advances in Fmoc solid-phase peptide synthesis. *J Pept Sci*. 2016;22(1):4–27. <https://doi.org/10.1002/psc.2836>
- Böttger R, Hoffmann R, Knappe D. Differential stability of therapeutic peptides with different proteolytic cleavage sites in blood, plasma and serum. *PloS One*. 2017;12(6):e0178943. <https://doi.org/10.1371/journal.pone.0178943>
- Boulangier J, Huesca M, Arab S, Lingwood CA. Universal method for the facile production of glycolipid/lipid matrices for the affinity purification of binding ligands. *Anal Biochem*. 1994; 217(1):1–6. <https://doi.org/10.1006/abio.1994.1075>
- Boutureira O, Bernardes GJL. Advances in chemical protein modification. *Chem Rev*. 2015;115(5):2174–95. <https://doi.org/10.1021/cr500399p>
- Brigotti M, Caprioli A, Tozzi AE, Tazzari PL, Ricci F, Conte R, et al. Shiga toxins present in the gut and in the polymorphonuclear leukocytes circulating in the blood of children with hemolytic-uremic syndrome. *J Clin Microbiol*. 2006;44(2):313–7. <https://doi.org/10.1128/JCM.44.2.313-317.2006>
- Chen YQ, Zhang SQ, Li BC, Qiu W, Jiao B, Zhang J, et al. Expression of a cytotoxic cationic antibacterial peptide in *Escherichia coli* using two fusion partners. *Protein Expr Purif*. 2008;57(2): 303–11. <https://doi.org/10.1016/j.pep.2007.09.012>
- Conrady DG, Flagler MJ, Friedmann DR, Vander Wielen BD, Kovall RA, Weiss AA, et al. Molecular basis of differential B-pentamer stability of Shiga toxins 1 and 2. *PloS One*. 2010; 5(12):e15153. <https://doi.org/10.1371/journal.pone.0015153>
- Cortez-Retamozo V, Lauwereys M, Hassanzadeh GG, Gobert M, Conrath K, Muyldermans S, et al. Efficient tumor targeting by single-domain antibody fragments of camels. *Int J Cancer*. 2002;98(3):456–62. <https://doi.org/10.1002/ijc.10212>
- Desai TJ, Toombs JE, Minna JD, Brekken RA, Udugamasooriya DG. Identification of lipid-phosphatidylserine (PS) as the target of unbiasedly selected cancer specific peptide-peptoid hybrid PPS1. *Oncotarget*. 2016;7(21):30678–90. <https://doi.org/10.18632/oncotarget.8929>
- Deslouches B, Di YP. Antimicrobial peptides with selective antitumor mechanisms: prospect for anticancer applications. *Oncotarget*. 2017;8(28):46635–51. <https://doi.org/10.18632/oncotarget.16743>
- Dolezal O, Pearce LA, Lawrence LJ, McCoy AJ, Hudson PJ, Kortt AA. ScFv multimers of the anti-neuraminidase antibody NC10: shortening of the linker in single-chain Fv fragment assembled in V(L) to V(H) orientation drives the formation of dimers, trimers, tetramers and higher molecular mass

- multimers. *Proteins*. 2000;13(8):565–74. <https://doi.org/10.1093/protein/13.8.565>
- El Alaoui A, Schmidt F, Amessou M, Sarr M, Decaudin D, Florent J-C, et al. Shiga toxin-mediated retrograde delivery of a topoisomerase I inhibitor prodrug. *Angew Chem Int Ed Engl*. 2007;46(34):6469–72. <https://doi.org/10.1002/anie.200701270>
- Geyer PE, Maak M, Nitsche U, Perl M, Novotny A, Slotta-Huspenina J, et al. Gastric adenocarcinomas express the glycosphingolipid Gb3/CD77: targeting of gastric cancer cells with Shiga toxin B-subunit. *Mol Cancer Ther*. 2016;15(5):1008–17. <https://doi.org/10.1158/1535-7163.MCT-15-0633>
- Gifford JL, Hunter HN, Vogel HJ. Lactoferricin: a lactoferrin-derived peptide with antimicrobial, antiviral, antitumor and immunological properties. *Cell Mol Life Sci*. 2005;62(22):2588–98. <https://doi.org/10.1007/s00018-005-5373-z>
- Grissenberger S, Riedl S, Rinner B, Leber R, Zweytick D. Design of human lactoferricin derived antitumor peptides-activity and specificity against malignant melanoma in 2D and 3D model studies. *Biochim Biophys Acta Biomembr*. 2020;1862(8):183264. <https://doi.org/10.1016/j.bbamem.2020.183264>
- Guerra JR, Cárdenas AB, Ochoa-Zarzosa A, Meza JL, Umaña Pérez A, Fierro-Medina R, et al. The tetrameric peptide LfcinB (20-25)(4) derived from bovine lactoferricin induces apoptosis in the MCF-7 breast cancer cell line. *RSC Adv*. 2019;9(36):20497–504. <https://doi.org/10.1039/c9ra04145a>
- Ji X, Zhang P, Armstrong RN, Gilliland GL. The three-dimensional structure of a glutathione S-transferase from the mu gene class. Structural analysis of the binary complex of isoenzyme 3-3 and glutathione at 2.2-Å resolution. *Biochemistry*. 1992;31(42):10169–84. <https://doi.org/10.1021/bi00157a004>
- Ko JH, Maynard HD. A guide to maximizing the therapeutic potential of protein-polymer conjugates by rational design. *Chem Soc Rev*. 2018;47(24):8998–9014. <https://doi.org/10.1039/c8cs00606g>
- Kurhade SE, Ross P, Gao FP, Farrell MP. Lectin drug conjugates targeting high mannose N-Glycans. *Chembiochem*. 2022;23(19):e202200266. <https://doi.org/10.1002/cbic.202200266>
- Law B, Quinti L, Choi Y, Weissleder R, Tung C-H. A mitochondrial targeted fusion peptide exhibits remarkable cytotoxicity. *Mol Cancer Ther*. 2006;5(8):1944–9. <https://doi.org/10.1158/1535-7163.MCT-05-0509>
- Liu G-H, Chen T, Zhang X, Ma X-L, Shi H-S. Small molecule inhibitors targeting the cancers. *MedComm*. 2022;3(4):e181. <https://doi.org/10.1002/mco2.181>
- Maxian T, Gerlitz L, Riedl S, Rinner B, Zweytick D. Effect of L- to D-amino acid substitution on stability and activity of antitumor peptide RDP215 against human melanoma and glioblastoma. *Int J Mol Sci*. 2021;22(16):8469. <https://doi.org/10.3390/ijms22168469>
- Nakajima H, Katagiri YU, Kiyokawa N, Taguchi T, Suzuki T, Sekino T, et al. Single-step method for purification of Shiga toxin-1 B subunit using receptor-mediated affinity chromatography by globotriaosylceramide-conjugated octyl sepharose CL-4B. *Protein Expr Purif*. 2001;22(2):267–75. <https://doi.org/10.1006/prep.2001.1449>
- Nejadmoghaddam M-R, Minai-Tehrani A, Ghahremanzadeh R, Mahmoudi M, Dinarvand R, Zarnani A-H. Antibody-drug conjugates: possibilities and challenges. *Avicenna J Med Biotechnol*. 2019;11(1):3–23.
- Ngo S, Guo Z. Key residues for the oligomerization of Aβ42 protein in Alzheimer's disease. *Biochem Biophys Res Commun*. 2011;414(3):512–6. <https://doi.org/10.1016/j.bbrc.2011.09.097>
- Ochiishi T, Doi M, Yamasaki K, Hirose K, Kitamura A, Urabe T, et al. Development of new fusion proteins for visualizing amyloid-β oligomers in vivo. *Sci Rep*. 2016;6:22712. <https://doi.org/10.1038/srep22712>
- Pan X, Xu J, Jia X. Research Progress evaluating the function and mechanism of anti-tumor peptides. *Cancer Manag Res*. 2020;12:397–409. <https://doi.org/10.2147/CMAR.S232708>
- Parker MW, Lo Bello M, Federici G. Crystallization of glutathione S-transferase from human placenta. *J Mol Biol*. 1990;213(2):221–2. [https://doi.org/10.1016/s0022-2836\(05\)80183-4](https://doi.org/10.1016/s0022-2836(05)80183-4)
- Pasupuleti R, Rosato F, Kolanovic D, Makshakova ON, Römer W, Wiltschi B. Genetic code expansion in *E. coli* enables production of a functional “ready-to-click” T cell receptor-specific scFv. *N Biotechnol*. 2023;76:127–37. <https://doi.org/10.1016/j.nbt.2023.05.007>
- Pozsgay V, Trinh L, Shiloach J, Robbins JB, Donohue-Rolfe A, Calderwood SB. Purification of subunit B of Shiga toxin using a synthetic trisaccharide-based affinity matrix. *Bioconjug Chem*. 1996;7(1):45–55. <https://doi.org/10.1021/bc9500711>
- Ran S, Downes A, Thorpe PE. Increased exposure of anionic phospholipids on the surface of tumor blood vessels. *Cancer Res*. 2002;62(21):6132–40.
- Riedl S, Leber R, Rinner B, Schaidler H, Lohner K, Zweytick D. Human lactoferricin derived di-peptides deploying loop structures induce apoptosis specifically in cancer cells through targeting membranous phosphatidylserine. *Biochim Biophys Acta*. 2015;1848(11 Pt A):2918–31. <https://doi.org/10.1016/j.bbamem.2015.07.018>
- Riedl S, Rinner B, Asslaber M, Schaidler H, Walzer S, Novak A, et al. In search of a novel target - phosphatidylserine exposed by non-apoptotic tumor cells and metastases of malignancies with poor treatment efficacy. *Biochim Biophys Acta*. 2011;1808(11):2638–45. <https://doi.org/10.1016/j.bbamem.2011.07.026>
- Riedl S, Rinner B, Schaidler H, Liegl-Atzwanger B, Meditz K, Preishuber-Pflügl J, et al. In vitro and in vivo cytotoxic activity of human lactoferricin derived antitumor peptide R-DIM-P-LF11-334 on human malignant melanoma. *Oncotarget*. 2017;8(42):71817–32. <https://doi.org/10.18632/oncotarget.17823>
- Riedl S, Rinner B, Schaidler H, Lohner K, Zweytick D. Killing of melanoma cells and their metastases by human lactoferricin derivatives requires interaction with the cancer marker phosphatidylserine. *Biometals*. 2014;27(5):981–97. <https://doi.org/10.1007/s10534-014-9749-0>
- Rosato F, Pasupuleti R, Tomisch J, Meléndez AV, Kolanovic D, Makshakova ON, et al. A bispecific, crosslinking lectin body activates cytotoxic T cells and induces cancer cell death. *J Transl Med*. 2022;20(1):578. <https://doi.org/10.1186/s12967-022-03794-w>
- Sadeghian-Rizi T, Ebrahimi A, Moazzen F, Yousefian H, Jahanian-Najafabadi A. Improvement of solubility and yield of recombinant protein expression in *E. coli* using a two-step system. *Res Pharm Sci*. 2019;14(5):400–7. <https://doi.org/10.4103/1735-5362.268200>
- Sarfo K, Moorhead GBG, Turner RJ. A novel procedure for separating small peptides on polyacrylamide gels. *Lett Pept Sci*. 2003;10(2):127–33. <https://doi.org/10.1023/B:LIPS.0000032383.40916.e2>

- Skosyrev VS, Kuleskiy EA, Yakhnin AV, Temirov YV, Vinokurov LM. Expression of the recombinant antibacterial peptide sarcotoxin IA in *Escherichia coli* cells. *Protein Expr Purif*. 2003;28(2):350–6. [https://doi.org/10.1016/s1046-5928\(02\)00697-6](https://doi.org/10.1016/s1046-5928(02)00697-6)
- Stafford JH, Thorpe PE. Increased exposure of phosphatidylethanolamine on the surface of tumor vascular endothelium. *Neoplasia*. 2011;13(4):299–308. <https://doi.org/10.1593/neo.101366>
- Vaughan HJ, Green JJ, Tzeng SY. Cancer-targeting nanoparticles for combinatorial nucleic acid delivery. *Adv Mater*. 2020;32(13):e1901081. <https://doi.org/10.1002/adma.201901081>
- Vlieghe P, Lisowski V, Martinez J, Khrestchatskiy M. Synthetic therapeutic peptides: science and market. *Drug Discov Today*. 2010;15(1–2):40–56. <https://doi.org/10.1016/j.drudis.2009.10.009>
- Wimley WC, White SH. Experimentally determined hydrophobicity scale for proteins at membrane interfaces. *Nat Struct Biol*. 1996;3(10):842–8. <https://doi.org/10.1038/nsb1096-842>
- Wingfield PT. Overview of the purification of recombinant proteins. *Curr Protoc Protein Sci*. 2015;80:6.1.1–6.1.35. <https://doi.org/10.1002/0471140864.ps0601s80>
- Wodlej C, Riedl S, Rinner B, Leber R, Drechsler C, Voelker DR, et al. Interaction of two antitumor peptides with membrane lipids - influence of phosphatidylserine and cholesterol on specificity for melanoma cells. *PloS One*. 2019;14(1):e0211187. <https://doi.org/10.1371/journal.pone.0211187>
- Wußmann M, Groeber-Becker FK, Riedl S, Alihodzic D, Padaric D, Gerlitz L, et al. In model, in vitro and in vivo killing efficacy of antitumor peptide RDP22 on MUG-Mel2, a patient derived cell line of an aggressive melanoma metastasis. *Biomedicines*. 2022;10(11):2961. <https://doi.org/10.3390/biomedicines10112961>
- Xie M, Liu D, Yang Y. Anti-cancer peptides: classification, mechanism of action, reconstruction and modification. *Open Biol*. 2020;10(7):200004. <https://doi.org/10.1098/rsob.200004>
- Zhang X, Zhang Y. Applications of azide-based bioorthogonal click chemistry in glycobiology. *Molecules*. 2013;18(6):7145–59. <https://doi.org/10.3390/molecules18067145>
- Zhao HL, Yao XQ, Xue C, Wang Y, Xiong XH, Liu ZM. Increasing the homogeneity, stability and activity of human serum albumin and interferon-alpha2b fusion protein by linker engineering. *Protein Expr Purif*. 2008;61(1):73–7. <https://doi.org/10.1016/j.pep.2008.04.013>
- Zhong L, Li Y, Xiong L, Wang W, Wu M, Yuan T, et al. Small molecules in targeted cancer therapy: advances, challenges, and future perspectives. *Signal Transduct Target Ther*. 2021;6(1):201. <https://doi.org/10.1038/s41392-021-00572-w>
- Zorko M, Japelj B, Hafner-Bratkovic I, Jerala R. Expression, purification and structural studies of a short antimicrobial peptide. *Biochim Biophys Acta*. 2009;1788(2):314–23. <https://doi.org/10.1016/j.bbamem.2008.10.015>
- Zweytick D, Pabst G, Abuja PM, Jilek A, Blondelle SE, Andrä J, et al. Influence of N-acylation of a peptide derived from human lactoferricin on membrane selectivity. *Biochim Biophys Acta*. 2006;1758(9):1426–35. <https://doi.org/10.1016/j.bbamem.2006.02.032>

## SUPPORTING INFORMATION

Additional supporting information can be found online in the Supporting Information section at the end of this article.

**How to cite this article:** Pasupuleti R, Riedl S, Saltor Núñez L, Karava M, Kumar V, Kourist R, et al. Lectin-anticancer peptide fusion demonstrates a significant cancer-cell-selective cytotoxic effect and inspires the production of “clickable” anticancer peptide in *Escherichia coli*. *Protein Science*. 2023;32(12):e4830. <https://doi.org/10.1002/pro.4830>